ARTICLE NO. 80-4059

C 80-071

Application of the Fast Fourier Transform to Two-Dimensional Wind Tunnel Wall Interference

00032
20016
20018

M. Mokry* and L.H. Ohman†
National Research Council Canada, Ottawa, Ontario

Wall interference corrections are evaluated from experimental wind tunnel wall pressure distributions using the Fourier solution for the Dirichlet problem in a rectangle. The series coefficients are computed by the fast Fourier transform, making the method very efficient and suitable as a practical wall correction procedure for two-dimensional wind tunnel data. The method is applicable to arbitrary subcritical wind tunnel walls and the knowledge of their cross-flow properties is not required. A practical example is given for the BGK 1 airfoil, tested at supercritical flow conditions in the 20% perforated wall test section of the NAE high Reynolds number wind tunnel.

Nomenclature

a,b	= sides of rectangle R in the ξ,η plane
A	= cross-sectional area of the airfoil, non-dimensionalized by c^2
$A_k{}^{(\,)},B_k{}^{(\,)}$	= series coefficients
c	= chord length of the airfoil
C_L	= lift coefficient of the airfoil
C_p	= pressure coefficient
$f^{(\,)},g^{(\,)}$	= boundary values of u
f,g	= contributions to u from $f^{(\,)},g^{(\,)}$
h	= test section height
m,n	= integer powers of 2
M	= stream Mach number
P	= porosity parameter
r	$=(x^2+y^2)^{1/2}$
R	= interior of the control rectangle
R_c	= Reynolds number based on chord length
S	= smoothing factor
t	= computation time
u,v	= reduced components of wall interference velocity
x,y	= physical coordinates
α	= geometrical angle of attack
β	$=(1-M^2)^{1/2}$
γ	= vortex strength
δR	= boundary of rectangle R
ΔM	= Mach number correction
$\Delta\alpha$	= angle of attack correction
κ	= ratio of specific heats (1.4 for air)
μ	= doublet strength
μ_k,ν_k	= eigenvalues
ξ,η	= reduced coordinates
ϕ	= disturbance velocity potential
ϕ_F	= "free air" part of ϕ
ϕ_W	= "wall interference" part of ϕ
ψ	= flow angle

Subscripts

0	= flow angle reference station
$1,2$	= rectangle boundaries

Received June 15, 1979; revision received Dec. 17, 1979.

Index categories: Testing, Flight and Ground; Subsonic Flow; Transonic Flow.

*Associate Research Officer, High Speed Aerodynamics Laboratory. Member AIAA.

†Head, High Speed Aerodynamics Laboratory. Member AIAA.

Introduction

THE difficulties connected with measuring flows through ventilated wind tunnel walls and with the mathematical modeling of flows involving associated complex boundary conditions have led to numerous techniques for the evaluation of wall interference effects on tested models by the integration of measured wall pressures; for some more recent developments see Refs. 1-9. The problem of assessing the tunnel interference by using boundary measurements has also been addressed by Lo,[10] but his method falls into a different category since it, in addition to pressures, also utilizes the boundary distribution of flow angles. With a more complete set of boundary values it is possible to formulate the wall interference problem more exactly; on the other hand, an accurate measurement of flow angles in the disturbed environment of ventilated wind tunnel walls is quite a difficult technical task, so that the methods based upon pressure measurements only would likely have a wider applicability.

The present method is based upon a principle similar to that described by Capelier, Chevallier, and Bouniol,[3] the major difference being in the selection of boundaries and implementation of the integration of wall pressures. It is applicable to arbitrary test section walls operated at subcritical flow conditions and the knowledge of cross-flow properties of the walls is not required. Since in the flow regions adjacent to the walls the level of pressure disturbances is very low, local linearization can be applied to the velocity potential up to very high subsonic Mach numbers of the stream. Upon applying the compressibility transformation, the x component of stream velocity can be retrieved from the measured wall pressures as the solution of a Dirichlet problem and the y component is obtained as its harmonic conjugate. Since in the latter operation the integration constant is arbitrary, the value of the y component of velocity (or the flow direction) at an arbitrary field point has to be specified.

In Ref. 3, the solution is constructed for a wind tunnel represented by an infinite strip (Fig. 1a) and both components of velocity are obtained in one operation using the conformal mapping of the strip onto a half-plane. The wall interference corrections are presented in terms of infinite integrals along the walls. However, since the pressures can be measured only over a finite length of the test section, the boundary values have to be extrapolated to infinitely distant upstream and downstream points.

The present paper utilizes the Fourier solution of the Dirichlet problem for a finite rectangular region (Fig. 1b). This, in principle, requires that the static pressure be measured across the two end planes in addition to the floor and ceiling pressures. However, if the latter are measured sufficiently far upstream and downstream of the model location, a simple interpolation of end plane pressures will

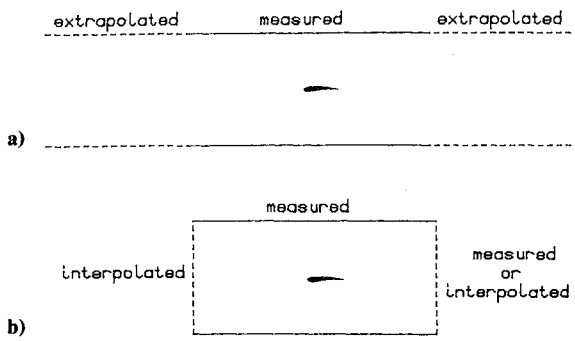

Fig. 1 Determination of boundary pressures: a) infinite strip, b) rectangle.

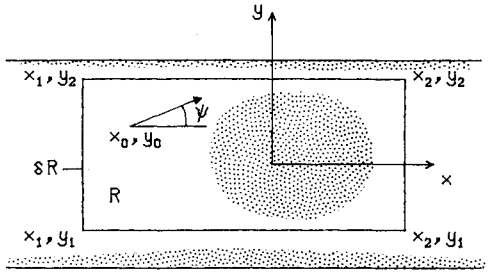

Fig. 2 Coordinate system.

suffice. Performing the integration of pressure distributions by the fast Fourier transform (FFT) technique, the wall interference corrections are obtained in terms of finite series of pressures at discrete points, equally spaced along the boundary. The correctness of the method is demonstrated with a theoretical example and its application to some actual experimental cases is described.

Governing Equations

The quarter-chord of the airfoil is at $x=y=0$ and the wind tunnel flow is investigated in the rectangle $R=\{(x,y)\,|\,x_1<x<x_2, y_1<y<y_2\}$ located inside a two-dimensional test section (Fig. 2). Assuming that on the boundary δR of the rectangle the flow is nearly parallel to the undisturbed flow far upstream and the pressure coefficient C_p is small and subcritical, the disturbance velocity potential ϕ satisfies near δR the linearized equation

$$\beta^2 \frac{\partial^2 \phi}{\partial x^2}(x,y) + \frac{\partial^2 \phi}{\partial y^2}(x,y) = 0 \tag{1}$$

and

$$C_p(x,y) = -2\frac{\partial \phi}{\partial x}(x,y) \tag{2}$$

In the linearized flow region (unshaded area between the walls in Fig. 2) we can use the decomposition

$$\phi(x,y) = \phi_W(x,y) + \phi_F(x,y) \tag{3}$$

where ϕ_W satisfies Eq. (1) in $R \cup \delta R$ and ϕ_F satisfies Eq. (1) in the infinite region exterior to R (also in the intersection of the linearized flow region and R) and obeys the farfield condition

$$\frac{\partial \phi_F}{\partial x}\bigg|_{r\to\infty} = \frac{\partial \phi_F}{\partial y}\bigg|_{r\to\infty} = 0 \tag{4}$$

Using a Laurent series expansion of the complex disturbance velocity in the (doubly connected) linearized flow region, we obtain from the principal part of the series the following approximation to ϕ_F:

$$\phi_F(x,y) = -\frac{\gamma}{2\pi}\operatorname{atan}\frac{\beta y}{x} + \frac{\mu}{2\pi\beta}\frac{x}{x^2+(\beta y)^2} + \ldots \tag{5}$$

The strength γ of the vortex term is the circulation around δR; from the Joukowski theorem

$$\gamma = \tfrac{1}{2} c C_L \tag{6}$$

For attached viscous flows the discharge through δR (wake effect) is negligible, and hence Eq. (5) does not contain a source term. Its presence would be justified for the case of airfoils in stall conditions, but then the practical applicability of the present theory has to be questioned as a whole, since it is seldom possible to keep the flow truly two-dimensional.

The displacement effect is represented by the doublet term, whose strength μ for incompressible flow is the cross-sectional area of the airfoil, or

$$\mu = c^2 A \tag{7}$$

For compressible flow, μ includes additional terms (cf. Ref. 11) but they are not easy to estimate if only the boundary pressure measurement is available. Fortunately, for lifting flows the vortex term usually dominates the farfield, so that the error due to evaluating μ from Eq. (7) is relatively small.

In wall interference theory the derivatives $\partial\phi_W/\partial x$ and $\partial\phi_W/\partial y$, calculated at the position of the airfoil, are interpreted as the corrections to the x and y components of the wind tunnel stream velocity. This concept proves to be valid if the airfoil is infinitesimal or if $\partial\phi_W/\partial x$ and $\partial\phi_W/\partial y$ are constants in R. The former case is obviously of little practical interest; in the latter case ϕ_W satisfies Eq. (1) in the entire plane and the components of disturbance velocity have the limits

$$\frac{\partial \phi}{\partial x}\bigg|_{r\to\infty} = \frac{\partial \phi_W}{\partial x}(0,0)$$

$$\frac{\partial \phi}{\partial y}\bigg|_{r\to\infty} = \frac{\partial \phi_W}{\partial y}(0,0) \tag{8}$$

However, if the higher derivatives of ϕ_W are nonzero, then the first derivatives of ϕ_W cannot be bounded in the entire plane (Liouville's theorem) and there is not an equivalent free airflow condition corresponding to the one the airfoil is subjected to in the wind tunnel. A less strict view, often utilized in practice, is that the higher derivatives of ϕ_W cause a distortion of the flow in the wind tunnel that does not exist in free air. Depending upon the magnitude of this distortion and accuracy requirements for the measurement, we can speak of the "correctable" or "uncorrectable" wind tunnel test (for more discussion, see Ref. 1). In the present paper we restrict ourselves to cases where the flow distortion is kept within acceptable limits by suitable choice of the open area ratio of the test section walls and where the wall interference effect can be approximated by Eqs. (8).

Fourier Solution of the Wall Interference Problem

In order to calculate the derivatives of ϕ_W, we first use the transformation

$$\xi = \frac{1}{\beta}(x - x_1)$$

$$\eta = y - y_1 \tag{9}$$

which reduces Eq. (1) to the Laplace equation. In view of the differentiability of harmonic functions, the reduced x component of interference velocity

$$u(\xi,n)=\frac{\partial\phi_W}{\partial\xi}(x,y)=\beta\frac{\partial\phi_W}{\partial x}(x,y) \tag{10}$$

satisfies

$$\frac{\partial^2 u}{\partial\xi^2}(\xi,n)+\frac{\partial^2 u}{\partial\eta^2}(\xi,\eta)=0 \tag{11}$$

in the region $0<\xi<a$, $0<\eta<b$, where

$$a=\frac{1}{\beta}(x_2-x_1)$$
$$b=y_2-y_1 \tag{12}$$

Using Eqs. (2) and (3), the boundary values

$$\begin{aligned} u(\xi,0)&=f^{(1)}(\xi), \quad 0<\xi<a\\ u(\xi,b)&=f^{(2)}(\xi), \quad 0<\xi<a\\ u(0,\eta)&=g^{(1)}(\eta), \quad 0<\eta<b\\ u(a,\eta)&=g^{(2)}(\eta), \quad 0<\eta<b \end{aligned} \tag{13}$$

are obtained from measured boundary pressure distributions as

$$u(\xi,\eta)=-\beta[\tfrac{1}{2}C_p(x,y)+\frac{\partial\phi_F}{\partial x}(x,y)] \tag{14}$$

In the case where the pressures across the stream are not available, but the pressures along the wind tunnel walls are measured sufficiently far upstream and downstream, the values $g^{(\ )}$ can be approximated using (linear) interpolation of the corner values of $f^{(\ )}$.

Equations (11) and (13) specify a Dirichlet problem that can be solved in the closed form by the Fourier method (e.g., see Ref. 12). The solution, adapted for the application of the fast Fourier transform, reads

$$u(\xi,\eta)=f(\xi,\eta)+g(\xi,\eta) \tag{15}$$

where

$$f(\xi,\eta)=\sum_{k=1}^{m/2-1}\sin\mu_k\xi\left[A_k{}^{(1)}\frac{\sinh\mu_k(b-\eta)}{\sinh\mu_k b}+A_k{}^{(2)}\frac{\sinh\mu_k\eta}{\sinh\mu_k b}\right]$$

$$g(\xi,\eta)=\sum_{k=1}^{n/2-1}\sin\nu_k\eta\left[B_k{}^{(1)}\frac{\sinh\nu_k(a-\xi)}{\sinh\nu_k a}+B_k{}^{(2)}\frac{\sinh\nu_k\xi}{\sinh\nu_k a}\right] \tag{16}$$

and

$$\mu_k=\frac{k\pi}{a}$$
$$\nu_k=\frac{k\pi}{b} \tag{17}$$

The series coefficients are

$$A_k{}^{(\ )}=\frac{2}{m}\sum_{j=0}^{m-1}f^{(\ )}[a(2j+1)/m]\sin(2\pi jk/m)$$

$$B_k{}^{(\ )}=\frac{2}{n}\sum_{j=0}^{n-1}g^{(\ )}[b(2j+1)/n]\sin(2\pi jk/n) \tag{18}$$

where $f^{(\ )}$ and $g^{(\ )}$ stand for the odd extensions of the boundary functions of Eq. (13) on the intervals $0<\xi<2a$ and $0<\eta<2b$, respectively. The solution [Eq. (15)] tends to the exact solution if $m,n\to\infty$; for the best efficiency of the fast Fourier transform, m and n should be selected as integer powers of 2.

Wall Interference Corrections

By differentiating the adiabatic relation between velocity and Mach number, the Mach number correction is obtained as

$$\Delta M=(1+\frac{\kappa-1}{2}M^2)M\frac{\partial\phi_W}{\partial x}(0,0) \tag{19}$$

where, according to Eqs. (9) and (10)

$$\frac{\partial\phi_W}{\partial x}(0,0)=\frac{1}{\beta}u(-\frac{x_1}{\beta},-y_1) \tag{20}$$

The angle of attack correction (in radians)

$$\Delta\alpha=\frac{\partial\phi_W}{\partial y}(0,0) \tag{21}$$

can be expressed in terms of the function

$$v(\xi,\eta)=\int\frac{\partial u}{\partial\eta}(\xi,\eta)\,d\xi=-\int\frac{\partial u}{\partial\xi}(\xi,\eta)\,d\eta \tag{22}$$

which is determined from Eqs. (15) and (16) to within an arbitrary constant. Using Eqs. (9) and (10)

$$\begin{aligned}&\frac{\partial\phi_W}{\partial y}(0,0)-\frac{\partial\phi_W}{\partial y}(x_0,y_0)\\ &=v(-\frac{x_1}{\beta},-y_1)-v(\frac{x_0-x_1}{\beta},y_0-y_1)\end{aligned}$$

If the reference point x_0,y_0 is selected inside the linearized flow region, we have from Eq. (3)

$$\frac{\partial\phi_W}{\partial y}(x_0,y_0)=\psi(x_0,y_0)-\frac{\partial\phi_F}{\partial y}(x_0,y_0)$$

where

$$\psi(x_0,y_0)=\frac{\partial\phi}{\partial y}(x_0,y_0) \tag{23}$$

denotes the flow angle (in radians), see Fig. 2. Consequently

$$\begin{aligned}\Delta\alpha=&v(-\frac{x_1}{\beta},-y_1)-v(\frac{x_0-x_1}{\beta},y_0-y_1)\\ &+\psi(x_0,y_0)-\frac{\partial\phi_F}{\partial y}(x_0,y_0)\end{aligned} \tag{24}$$

The only unknown term in Eq. (24) is the flow angle ψ at x_0,y_0, which has to be measured (yawmeter, laser velocimeter, etc.) or estimated by other means.

The evaluation of higher derivatives of ϕ_W in terms of u is straightforward and need not be described here. As discussed above, these derivatives are indicative of the residual distortion of the wind tunnel flow. Of particular interest are $\partial^2\phi_W/\partial x^2$ and $\partial^2\phi_W/\partial x\partial y$, representing the pressure gradient and streamline curvature respectively.

Applications of the Method

Following the same approach as in Ref. 3, the accuracy of the present method is first demonstrated for a theoretical porous wall wind tunnel, consisting of two infinite walls parallel with the x-axis and specified by the boundary condition.

$$P\frac{\partial\phi}{\partial x}(x,\pm h/2)\pm\frac{\partial\phi}{\partial y}(x,\pm h/2)=0$$

The upper (plus) signs refer to the upper wall, the lower (minus) signs to the lower wall, $h>0$ is the distance between the walls, and $P\geq 0$ is the porosity parameter. Using the closed-form solution of Ref. 13, theoretical pressure distributions are generated along the boundary δR of an arbitrary interior rectangle (see Fig. 2) which contains the origin. In addition, the flow angle $\psi=\partial\phi/\partial y$ is calculated at $x_0=x_1, y_0=0$. These values are then picked up by the present method to evaluate the corrections ΔM and $\Delta\alpha$ and to compare them with their exact values according to Ref. 13.

The results in Table 1 are obtained for the following parameters: $h=6$ (arbitrary length units), $x_1=-8$, $x_2=4.5$, $y_1=-2.9$, $y_2=2.9$, $c=1$, $M=0.7$, $C_L=0.5$, and $A=0.1$. The selected porosity cases are: $P=0$ (solid walls), $P=1$ (typical porous walls), and $P=10^6$ (nearly open jet), for which the calculated values of $\psi(x_1,0)$ are 0.00677, 0.00020, and 0.00002 deg; respectively. It is seen that in the process of doubling m $(=n)$, the calculated corrections converge rapidly to exact ones in all three cases. The computation time t (on an IBM 370/3032) is roughly proportional to m $(=n)$, which is typical of a method based upon the fast Fourier transform.

The results in Table 2 correspond to the same input parameters, except that the boundary functions $g^{(\,)}$ are obtained by the interpolation of the corner values of $f^{(\,)}$. This case simulates more realistically an actual wind tunnel measurement, where the pressures across the stream are normally unavailable. Because of the error introduced by linear interpolation, the calculated corrections no longer converge to the exact six figure values. However, in view of the fact that experimentally Mach number and angle of attack are, at best, known to within ± 0.001 and ± 0.01 deg, respectively, such discrepancies are of no significance.

Having proved that the method produces correct values of ΔM and $\Delta\alpha$ for the theoretical wind tunnel case, it is reasonable to assume that it also performs well in real life situations, where measured pressure distributions along wind tunnel walls are supplied as input. To demonstrate its usefulness in a practical case, the method is applied to a recent series of tests on a 10 in. chord BGK 1 ("Shockless" No. 1) airfoil[14] tested at supercritical flow conditions in the 15×60 in. test section of the 5×5 ft blowdown wind tunnel at the National Aeronautical Establishment (NAE) in Ottawa. The pressures along the centerlines of the 20% perforated walls,‡ were measured by two 1 in. diameter static pressure tubes, designed specifically for this project. The tubes are 163 in. long and cover the whole length of the parallel section of the wind tunnel. The earlier used shorter rails[13] would not permit the application of the present method with sufficient accuracy. The upstream and downstream boundary values $g^{(\,)}$ are obtained by linear interpolation of the corner values of $f^{(\,)}$. The corrections ΔM and $\Delta\alpha$ are calculated using $x_1/c=-8$, $x_2/c=4.5$, $y_1/c=-2.9$, $y_2/c=2.9$, $c=10$ in., and $A=0.075$; the fast Fourier transform uses $m=n=2^8$. Results are presented for one test Mach number, $M=0.784$, and two lift coefficients, whose values are obtained by integration of measured airfoil pressure distributions.

‡The nominal porosity of perforated walls is 20.5%. However, by covering the center row of holes with the static tubes, the actual geometric porosity for the tests was 19.3%.

Usually, the measured wall pressures show quite a bit of scatter, the present cases being no exceptions, and smoothing by cubic splines[15,16] is applied here before calculating the values of the bounary functions $f^{(\,)}$. The amount of smoothing is controlled by the factor S, which for equal weights of all pressure points is defined as the sum of squared differences of the experimental and smoothed pressure coefficients. To illustrate the effect of smoothing on the resulting wall corrections, two rather extreme values of the smoothing factor are selected: $S=10^{-6}$ for which smoothing is practically equivalent to the interpolation by cubic splines, and $S=10^{-3}$ for which the curve is smoothed to such an extent that it almost has difficulties following the major trends of the experimental pressure distribution. From the results in Fig. 3 and 4 it is seen that ΔM is insensitive to S and that $\Delta\alpha$ is subject only to moderate variations, even when S differs as much as shown in the examples. This also indicates that the present method is relatively insensitive to experimental scatter or errors of isolated pressure points.

To support the corrections ΔM and $\Delta\alpha$ from Figs. 3 and 4, comparisons are made in Figs. 5 and 6 between airfoil pressure distributions measured in the wind tunnel (symbols) and the pressure distributions in free air (lines), computed by the Bauer-Garabedian-Korn-Jameson program.[17] In accordance with the computations of Ref. 17, used to compare theory with the earlier series of NAE tests of the same airfoil, the transition was set at 7% of the chord length. The location of actual transition for the present experimental data is not known, but it is believed to be close to the leading edge, because of the high Reynolds number, $R_c=21\times 10^6$ (based on chord).

In the computations, the angle of attack was allowed to float to produce the wind tunnel value of the lift coefficient C_L. In Figs. 5 and 6 the first case (solid line) is always computed for the nominal value of the tunnel Mach number, $M=0.784$, and the second case (dashed line) for the corrected

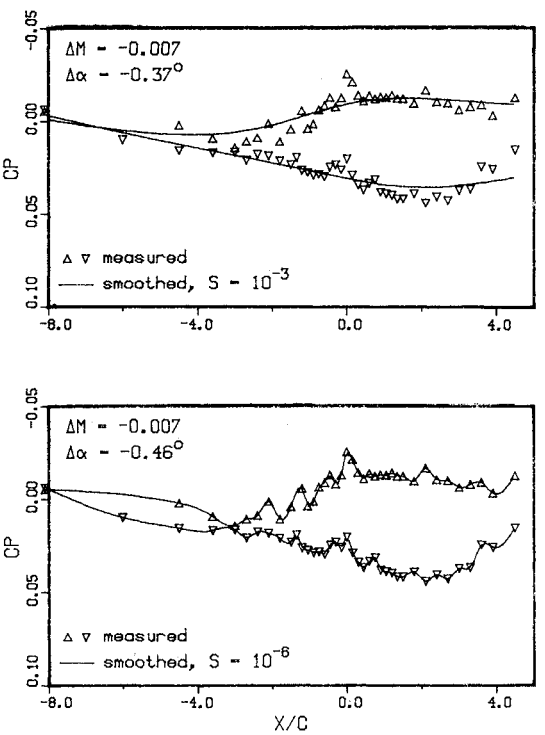

Fig. 3 Experimental and smoothed pressure distributions on perforated test section walls, $R_c=21\times 10^6$, $M=0.784$, $C_L=0.301$.

Table 1 Theoretical wall corrections using exact boundary values

	$P=0$		$P=1$		$P=10^6$		
$m=n$	ΔM	$\Delta\alpha$, deg	ΔM	$\Delta\alpha$, deg	ΔM	$\Delta\alpha$, deg	t,s
2	0.000000	−0.19674	−0.000002	−0.20393	−0.000001	−0.20422	0.005
4	0.001291	0.02537	0.000457	−0.00381	−0.000283	−1.04127	0.002
8	0.002844	0.04198	−0.000906	−0.60832	−0.001419	−1.20464	0.003
16	0.002857	0.00265	−0.000737	−0.69259	−0.001353	−1.18731	0.006
32	0.003018	0.00082	−0.000801	−0.71486	−0.001491	−1.19226	0.013
64	0.003056	0.00020	−0.000813	−0.72051	−0.001524	−1.19331	0.026
128	0.003066	0.00005	−0.000816	−0.72193	−0.001532	−1.19357	0.051
256	0.003069	0.00001	−0.000817	−0.72228	−0.001534	−1.19364	0.101
512	0.003069	0.00000	−0.000817	−0.72237	−0.001534	−1.19366	0.193
1024	0.003069	0.00000	−0.000817	−0.72239	−0.001535	−1.19366	0.379
2048	0.003069	0.00000	−0.000817	−0.72240	−0.001535	−1.19366	0.758
4096	0.003069	0.00000	−0.000817	−0.72240	−0.001535	−1.19366	1.529
Exact	0.003069	0.00000	−0.000817	−0.72240	−0.001535	−1.19366	

Table 2 Theoretical wall corrections using approximated boundary values

	$P=0$		$P=1$		$P=10^6$		
$m=n$	ΔM	$\Delta\alpha$, deg	ΔM	$\Delta\alpha$, deg	ΔM	$\Delta\alpha$, deg	t,s
2	−0.000002	−0.19735	0.000001	−0.20404	0.000001	−0.20259	0.003
4	0.001284	0.02537	0.000457	−0.00381	−0.000277	−1.04127	0.001
8	0.002834	0.04194	−0.000906	−0.60750	−0.001411	−1.20374	0.003
16	0.002848	0.00258	−0.000737	−0.69162	−0.001345	−1.18625	0.006
32	0.003008	0.00076	−0.000801	−0.71384	−0.001483	−1.19114	0.013
64	0.003047	0.00013	−0.000813	−0.71948	−0.001515	−1.19218	0.028
128	0.003056	0.00002	−0.000816	−0.72090	−0.001523	−1.19244	0.050
256	0.003059	0.00006	−0.000817	−0.72125	−0.001525	−1.19251	0.100
512	0.003059	0.00007	−0.000817	−0.72134	−0.001526	−1.19252	0.194
1024	0.003059	0.00007	−0.000817	−0.72136	−0.001526	−1.19253	0.379
2048	0.003059	0.00007	−0.000817	−0.72137	−0.001526	−1.19253	0.753
4096	0.003059	0.00007	−0.000817	−0.72137	−0.001526	−1.19253	1.533
Exact	0.003069	0.00000	−0.000817	−0.72240	−0.001535	−1.19366	

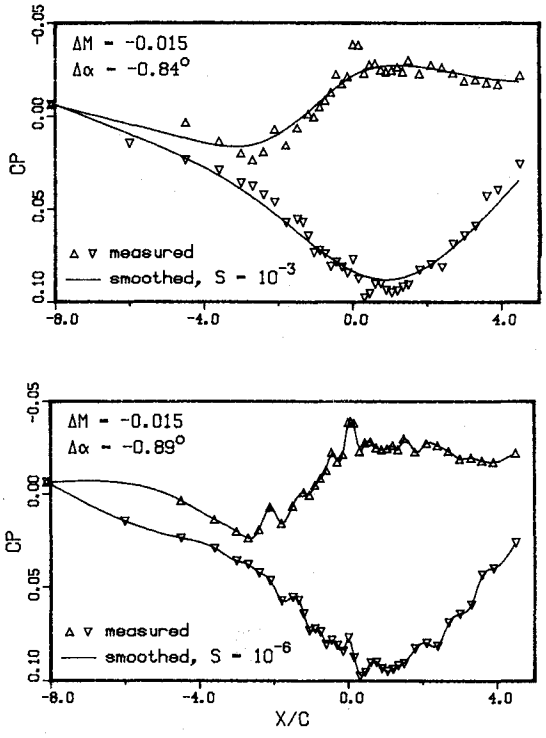

Fig. 4 Experimental and smoothed pressure distributions on perforated test section walls, $R_c = 21 \times 10^6$, $M = 0.784$, $C_L = 0.764$.

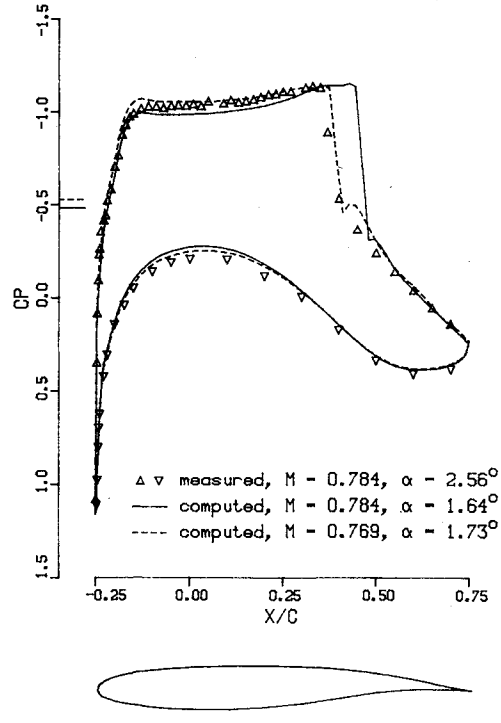

Fig. 6 Experimental and computed free air pressure distributions on BGK 1 airfoil, $R_c = 21 \times 10^6$, $C_L = 0.764$.

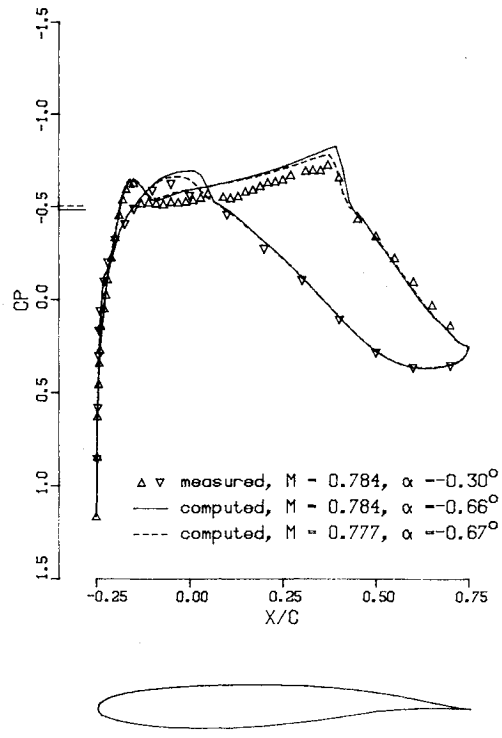

Fig. 5 Experimental and computed free air pressure distributions on BGK 1 airfoil, $R_c = 21 \times 10^6$, $C_L = 0.301$.

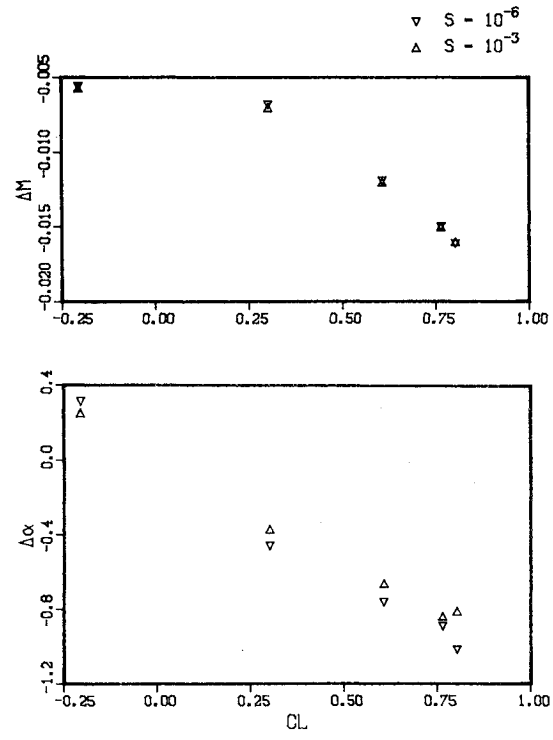

Fig. 7 Wall interference corrections for BGK 1 airfoil in 20% perforated test section, $R_c = 21 \times 10^6$, $M = 0.784$.

Mach number, $M = 0.784 + \Delta M$, where the correction value ΔM is taken from Figs. 3 and 4, respectively. It is seen that the application of the Mach number correction is very important for the correct prediction of the shock wave locations. Also, in Fig. 6 the overall agreement between the experimental and the computed surface pressures is greatly improved when the correction ΔM is applied. In the lower lift case (Fig. 5) the agreement theory and experiment is less spectacular due to the more complicated nature of the flow: there are two supercritical regions on the upper surface and one supercritical region on the lower surface. Apparently, the method of Ref. 17 underestimates the compression in the first shock on the upper surface and as a result the theoretical pressure is lower than the experimental one over a large part of the upper surface. However, in order to give this type of comparison more weight, the location of the actual transition would have to be known. Computations indicate that by displacing the transition point by 5% of the chord length, the theoretical shock waves in Fig. 6 move by about 1% of the chord length (in the same direction). Since the distance between the corrected (dashed line) and uncorrected (solid line) shock waves in Fig. 6 is about 7% of the chord length, the effect of transition certainly cannot be dismissed as negligible.

The differences between computed and experimental angles of attack, -0.37 deg in Fig. 5 and -0.83 deg in Fig. 6, are remarkably close to the values of $\Delta\alpha$ predicted from wall pressure distributions in Figs. 3 and 4. However, the following comment is appropriate. In the absence of the flow angle measurement (its importance during the wind tunnel tests had not been fully realized) the flow angle reference point was selected at $x_0 = x_l$, $y_0 = 0$. In Eq. (24) the value ψ was assumed to be a constant (independent of C_L), determined by the condition $\Delta\alpha = 0$ if $C_L = 0$. Since no measurements were made at $C_L = 0$, $\Delta\alpha$ was evaluated from a number of wall pressure distributions measured at different C_L (but the same M and R_c) and then shifting the curve vs C_L so as to pass through the origin of the corresponding graph. The result for the two values of the smoothing factor is shown in the lower portion of Fig. 7. Since the shift was found to be of significant magnitude (about -0.2 deg), this procedure is not suggested as a substitute for the flow angle measurement at a selected reference station. Problems of similar kind are not experienced with ΔM, since for its evaluation the wall pressures are sufficient. The values of ΔM are shown in the upper portion of Fig. 7; it can be again observed that ΔM is less sensitive to smoothing than $\Delta\alpha$.

The results in Fig. 7 further show that neither $\Delta\alpha$ nor ΔM are strictly linear functions of C_L as could be expected from classical wall interference theory. The strong dependence of ΔM on C_L may appear somewhat puzzling to those associating the ΔM correction with the blockage effect. However, this behavior is due to different inflow and outflow characteristics of the straight-hole perforated wall, as explained in Refs. 13 and 18. The smaller nonlinear trend in $\Delta\alpha$ vs C_L is somewhat obscured by the sensitivity to the choice of smoothing factor. It is worth noting that the last data point, i.e., the one corresponding to the highest C_L, is for a case of separated flow, which probably explains why it falls "out of line" in the lower graph.

The good correspondence between experiment and free air calculations in Figs. 5 and 6 indicates that the present measurements in the 20% perforated wall test section can be corrected using the values ΔM and $\Delta\alpha$ predicted from wall pressure distributions. It is also worth pointing out that Lock,[19] when looking for the best comparison of the NAE measured airfoil pressure distributions (earlier series of tests) with the computed ones by the VGK method,[20] applied a Mach number correction that fits the picture here presented.

Conclusions

A procedure based upon linear theory has been developed for the evaluation of wall interference corrections for an arbitrary two-dimensional test section whose walls are operated at subcritical flow conditions. As verified experimentally, local supercritical flow regions may exist on the tested airfoil.

An important feature of the method is that it utilizes measured boundary pressure distributions, but does not

require knowledge of the cross-flow properties of the walls. However, if the pressures on the upstream and downstream boundaries are not available, the wall pressures should be measured as far as the two-dimensional portion of the wind tunnel permits, allowing the upstream and downstream boundary values to be obtained by interpolation. The method is relatively insensitive to experimental scatter or type of smoothing applied.

The integration constant, needed for the evaluation of the angle of attack correction, should be obtained by measuring the flow angle at a selected reference point, sufficiently distant from the airfoil.

The utilization of the fast Fourier transform makes the method very efficient and suitable for routine correcting of two-dimensional wind tunnel measurements.

References

[1] Kemp, W.B., "Toward the Correctable-Interference Transonic Wind Tunnel," *Proceedings of AIAA 9th Aerodynamic Testing Conference,* June 1976, pp. 31-38.

[2] Aulehla, F., "Grenzen der Widerstandsbestimmung schlanker Körper in transsonischen Windkanälen," Messerschmitt-Bölkow-Blohm, UFE 1315 0, June 1976.

[3] Capelier, C., Chevallier, J.-P., and Bouniol, F., "Nouvelle méthode de correction des effets de parois en courant plan," *La Recherche Aérospatiale*, Jan.-Feb. 1978, pp. 1-11.

[4] Sawada, H., "A General Correction Method of the Interference in 2-Dimensional Wind Tunnels with Ventilated Walls," *Transactions of the Japan Society for Aeronautical and Space Sciences*, Vol. 21, 1978, pp. 57-68.

[5] Kemp, W.B., "Transonic Assessment of Two-Dimensional Wind Tunnel Wall Interference Using Measured Wall Pressures," *Advanced Technology Airfoil Research*, NASA Conference Publication 2045, March 1978, pp. 473-486.

[6] Stahara, S.S. and Spreiter, J.R., "A Transonic Wind Tunnel Interference Assessment—Axisymmetric Flows," AIAA Paper 79-0203, New Orleans, La., Jan. 1979.

[7] Hackett, J.E., Wilsden, D.J., and Lilley, D.E., "Estimation of Tunnel Blockage from Wall Pressure Signatures: A Review and Data Correlation," NASA CR-15, 224, March 1979.

[8] Blackwell, J.A., "Wind-Tunnel Blockage Correction for Two-Dimensional Transonic Flow," *Journal of Aircraft*, Vol. 16, April 1979, pp. 256-263.

[9] Murman, E.M., "A Correction Method for Transonic Wind Tunnel Wall Interference," AIAA Paper 79-1533, Williamsburg, Va., July 1979.

[10] Lo, C.F., "Tunnel Interference Assessment by Boundary Measurements," *AIAA Journal,* Vol. 16, April 1978, pp. 411-413.

[11] Klunker, E.B., "Contribution to Methods for Calculating the Flow about Thin Lifting Wings at Transonic Speeds—Analytic Expressions for the Far Field," NASA TN D-6530, Nov. 1971.

[12] Powers, D.L., *Boundary Value Problems*, Academic Press, New York 1972, pp. 113-117.

[13] Mokry, M., Peake, D.J., and Bowker, A.J., "Wall Interference on Two-Dimensional Supercritical Airfoils, Using Wall Pressure Measurements to Determine the Porosity Factors for Tunnel Floor and Ceiling," National Research Council Canada, Aeronautical Report LR-575, Feb. 1974.

[14] Kacprzynski, J.J., Ohman, L.H., Garabedian, P.R., and Korn, D.G., "Analysis of the Flow Past a Shockless Lifting Airfoil in Design and Off-Design Conditions," National Research Council Canada, Aeronautical Report LR-554, Nov. 1971.

[15] Reinsch, C.H., "Smoothing by Spline Functions," *Numerische Mathematik*, Vol. 10, 1967, pp. 177-183.

[16] Reinsch, C.H., "Smoothing by Spline Functions II," *Numerische Mathematik*, Vol. 16, 1971, pp. 451-454.

[17] Bauer, F., Garabedian, P., Korn, D., and Jameson, A., *Supercritical Wing Sections II*, Springer-Verlag, 1975, pp. 173-191 and 202-240.

[18] Lukasiewicz, J., "Effects of Boundary Layer and Geometry on Characteristics of Perforated Walls for Transonic Wind Tunnels," *Aerospace Engineering,* Vol. 20, April 1961, pp. 22-23 and 62-68.

[19] Lock, R.C., "Preliminary Note on the Tests in Commonwealth Wind Tunnels on the Supercritical Aerofoil 'Korn I' (BGK 1) with Comparisons with Theory," C.C. 766 Tech. 33, Commonwealth Advisory Aeronautical Research Council, May 1978.

[20] Collyer, M.R. and Lock, R.C., "Prediction of Viscous Effects in Steady Transonic Flow Past an Aerofoil," *The Aeronautical Quarterly*, Vol. 30, August 1979, pp. 485-505.